nature communications

Article

https://doi.org/10.1038/s41467-025-57494-2

Systematic biotechnological production of isoprenoid analogs with bespoke carbon skeletons

Received: 23 June 2024

Accepted: 24 February 2025

Published online: 01 March 2025

Check for updates

Lina Wang[1], Mads Rosenfeldt[1], Aikaterini Koutsaviti[2], Maria Harizani[2], Yong Zhao[1], Nattawat Leelahakorn[1], Axelle Frachon[3], Morten H. Raadam[1], Karel Miettinen[1], Irini Pateraki[1], Efstathia Ioannou[2] & Sotirios C. Kampranis[1]

Natural products are widely used as pharmaceuticals, flavors, fragrances, and cosmetic ingredients. Synthesizing and evaluating analogs of natural products can considerably expand their applications. However, the chemical synthesis of analogs of natural products is severely hampered by their highly complex structures. This is particularly evident in isoprenoids, the largest class of natural products. Here, we develop a yeast cell-based biocatalytic method that enables the systematic biotechnological production of analogs of different classes of isoprenoids (including monoterpenoids, sesquiterpenoids, triterpenoids, and cannabinoids) with additional carbons in their skeletons. We demonstrate the applicability of this approach through two proof-of-concept studies: the biosynthesis of the highly valued aroma ingredient ethyllinalool, and the production of cannabinoid analogs with improved cannabinoid receptor agonism. This method is simple, readily adaptable to any cell factory, and enables the tailored expansion of the isoprenoid chemical space to identify molecules with improved properties and the biotechnological production of valuable compounds.

Isoprenoids constitute the largest class of specialized metabolites found in terrestrial and marine organisms with over 180,000 known members (http://terokit.qmclab.com)[1]. They are widely used as pharmaceuticals (e.g., artemisinin, taxol, vinblastine, cannabinoids, QS-21 adjuvant)[2–9], flavors and fragrances (e.g., linalool, geraniol, limonene)[10,11], colorants (e.g., lycopene and β-carotene), and cosmetic ingredients (e.g., sclareol, santalol, patchoulol)[12]. The utilization of isoprenoids could be expanded further by producing isoprenoid analogs with improved or altered properties, opening up numerous new applications. However, the production of analogs has been greatly hindered by the structural complexity of isoprenoids, often featuring multiple chiral centers, which renders their chemical synthesis inefficient and frequently economically inviable. Thus, developing systematic and efficient methods for the production of analogs is essential to improve and expand the applications of this highly valuable group of natural products.

A cost-effective and sustainable solution to this problem would be the development of a biotechnological method based on cell factories, which can provide a scalable and green method for the production of isoprenoid analogs. However, efforts in this direction have, so far, made limited progress because they have been based on combinatorial biosynthesis strategies[13–16] that are confined to adding functional groups to existing isoprenoid core scaffolds but cannot radically alter the carbon backbone of the targeted structures. This is largely because the biosynthesis of isoprenoids is governed by the isoprene rule.

[1]Biochemical Engineering Group, Plant Biochemistry Section, Department of Plant and Environmental Sciences, University of Copenhagen, Thorvaldsensvej 40, 1871 Frederiksberg C, Denmark. [2]Section of Pharmacognosy and Chemistry of Natural Products, Department of Pharmacy, School of Health Sciences, National and Kapodistrian University of Athens, Panepistimiopolis Zografou, Athens 15771, Greece. [3]EvodiaBio ApS, Islevdalvej 211, 2610 Rødovre, Denmark. e-mail: eioannou@pharm.uoa.gr; soka@plen.ku.dk

According to this, all isoprenoids are built up from two five-carbon isoprene units, isopentenyl diphosphate (IPP) and dimethylallyl diphosphate (DMAPP). These two fundamental building blocks combine, by successive head-to-tail additions, into larger prenyl diphosphate precursors. Each of these precursors generates a distinct class of hydrocarbon backbones by the action of terpene synthases, i.e., geranyl diphosphate (GPP) gives rise to monoterpenes (C_{10}), farnesyl diphosphate (FPP) is converted to sesquiterpenes (C_{15}) and triterpenes (C_{30}), geranylgeranyl diphosphate (GGPP) produces diterpenes (C_{20}) and carotenoids (C_{40}). Subsequently, the terpene backbones are converted to a broad array of terpenoids by decorating enzymes, such as cytochrome P450s, dehydrogenases, or glycosyltransferases. Meroterpenoids, such as cannabinoids[3] and monoterpene indole alkaloids, are also derived from the same prenyl diphosphate building blocks. Almost all naturally produced isoprenoids discovered so far conform to the isoprene rule, with only a few exceptions[11,17–21].

Thus, to synthesize isoprenoids with carbon skeletons that do not conform to the isoprene rule, it is essential to bypass the dependence of isoprenoid biosynthesis on the C_5 precursors DMAPP and IPP. As these precursors are synthesized in all organisms mainly through the mevalonate and the methylerythritol phosphate pathways[22], surpassing this restriction requires establishing alternative biosynthetic routes that supply analogs of DMAPP or IPP (e.g., C_6 or C_7 precursors). Taking advantage of the established promiscuity of the isoprenoid biosynthetic enzymes[15,20,21,23–27], these alternative precursors could then be incorporated into non-canonical prenyl diphosphates and converted by downstream enzymes to modified terpene scaffolds. To establish an alternative pathway to synthesize DMAPP and IPP analogs, we explored the possibility of capitalizing on previous findings that reported that the alcohols prenol and isoprenol could be converted to DMAPP and IPP, respectively, by two successive phosphorylation reactions[28]. We hypothesized that using a similar approach, alcohols with structures analogous to prenol and isoprenol could be converted to the corresponding DMAPP and IPP analogs as long as a suitable pair of kinases could be identified. Such an alternative pathway could be incorporated in an engineered microorganism or plant cell to bypass the endogenous DMAPP- and IPP-supplying pathway and serve as the basis for the systematic biotechnological production of tailored isoprenoid analogs from defined building blocks.

Here, to implement this strategy, we select *Saccharomyces cerevisiae* (baker's yeast) as a platform, due to the ability of yeast to produce high-value isoprenoids and oxygenated derivatives economically and sustainably at an industrial scale[3,4,12,22,29]. We identify a kinase, *Arabidopsis thaliana* farnesol kinase (*At*FKI), which has high efficiency in converting isopentenol-like alcohols to the corresponding prenyl monophosphates, and introduce a second kinase, *A. thaliana* isopentenyl kinase (*At*IPK), to convert the *At*FKI-produced prenyl monophosphates to non-canonical diphosphate building blocks (Fig. 1). We then furnish this system with dedicated downstream pathways that convert the non-canonical building blocks to analogs of each of the different classes of isoprenoids, providing specific examples for the production of analogs of monoterpenoids, sesquiterpenoids, and triterpenoids. Finally, we demonstrate the applicability of this approach to produce isoprenoid analogs with improved properties by two proof-of-concept studies. First, we establish the biotechnological production of the high-value aroma compound ethyllinalool, which is a less volatile, sweeter, and less woody analog of natural linalool that cannot be found in nature and until now could only be chemically synthesized. In addition, we produce a set of linalool analogs with modified sensory characteristics. Second, we engineer yeast cells to produce cannabinoid analogs that have higher bioactivity compared to canonical cannabinoids and thus have promise for pharmacological applications. These two examples demonstrate the biotechnological potential of this method and establish a systematic approach for the bespoke expansion of the structural diversity of isoprenoids.

Results

Establishing an efficient isopentenol utilization pathway

For the proposed approach to be successful, it was essential to establish an efficient engineered pathway for the conversion of isopentenol-like alcohols to isoprenoid precursors, in yeast. Previous studies had identified kinases that can convert prenol or isoprenol to dimethyl phosphate (DMAP) or isopentenyl phosphate (IP)[23,28,30,31], but it was unclear whether these kinases were sufficiently efficient in yeast cells to support this approach. Therefore, we evaluated the efficiency of the previously identified kinases (i.e., *Sf*PhoN from *Shigella flexneri*, *Sc*CKI from *S. cerevisiae*, *Sc*EKI from *S. cerevisiae*, and *Ec*ThiM from *Escherichia coli*; Supplementary Table 1) in supporting the first phosphorylation reaction. For the second phosphorylation step, we selected *Arabidopsis thaliana* isopentenyl phosphate kinase (*At*IPK; Supplementary Table 1), which had been shown to produce IPP and DMAPP from IP and DMAP, respectively[28].

All the corresponding ORFs were cloned into the yeast high-copy number expression vectors pUUS[10] (for *Sf*PhoN, *Sc*CKI, *Sc*EKI, and *Ec*ThiM) and pHUS (for *At*IPK) under the inducible P_{GAL1} promoter and introduced into the W303-derived strain EGY48[32] (Supplementary Tables 2 and 3, Supplementary Data 1 and 2). EGY48 was selected because it does not contain any modifications boosting isoprenoid production through the endogenous mevalonate pathway, thus providing a clean background to evaluate the performance of the reconstructed pathway. Initially, we evaluated the selected kinases by supplying prenol and applying solid-phase micro-extraction (SPME) to analyze the produced volatile compounds by GC-MS. Typically, excess synthesis of GPP or FPP in yeast results in the emission of linalool or nerolidol, respectively, in the culture headspace[18,20,21,33]. However, we could not detect any additional isoprenoid compounds produced by yeast cultures supplemented with 0.01–1% prenol (Fig. 2a), suggesting that the enzymes previously reported were not sufficiently active in yeast cells. This prompted us to look for additional candidates for the first step of this pathway. We identified the enzyme farnesol kinase in *A. thaliana* (*At*FKI) as a suitable candidate because it had been shown to phosphorylate farnesol and to a lesser extent geraniol and geranylgeraniol[34], suggesting it may have relatively relaxed specificity and thus accept other prenol-like alcohols. To evaluate this candidate, we introduced *At*FKI and *At*IPK into EGY48 to generate strain LW05 (Supplementary Table 3). When prenol was added, this strain produced one major additional peak corresponding to the monoterpene alcohol linalool (Fig. 2a). This indicated that *At*FKI and *At*IPK can convert prenol to DMAPP, which, in turn, is combined with endogenous IPP by the yeast farnesyl diphosphate synthase Erg20p to produce GPP. When isoprenol was supplied instead of prenol, *At*FKI was again found to be the most efficient of all kinases evaluated for the first step, although in the case of isoprenol, *Ec*ThiM also supported considerable, albeit lower, linalool production (Fig. 2b).

After identifying *At*FKI as an efficient enzyme for the first step, we evaluated the performance of IPKs from different sources in the second phosphorylation reaction. We tested four enzymes, *At*IPK, *Mt*IPK from *Methanothermobacter thermautotrophicus*, *Ta*IPK from *Thermoplasma acidophilum*, and its variant *Ta*IPK(K204G)[35] (Supplementary Table 1), in combination with *At*FKI, for their ability to synthesize linalool in this system. We found that *At*IPK and *Ta*IPK(K204G) were equally efficient when prenol was supplied, while *At*IPK clearly stood out when isoprenol was used (Supplementary Fig. 1). Therefore, the combination of *At*FKI with *At*IPK was selected as the optimal configuration.

To further optimize the performance of the established pathway, we first aimed to improve the catalytic efficiency of *At*FKI. As *At*FKI possesses an *N*-terminal plastid transit peptide, we tested a truncated form of *At*FKI, named Δ65*At*FKI, lacking the first 65 amino acids predicted to correspond to the transit peptide by TargetP 2.0 (https://services.healthtech.dtu.dk/services/TargetP-2.0/). Compared to the full-length enzyme, the Δ65*At*FKI variant was 3.72 times more efficient

https://doi.org/10.1038/s41467-025-57494-2

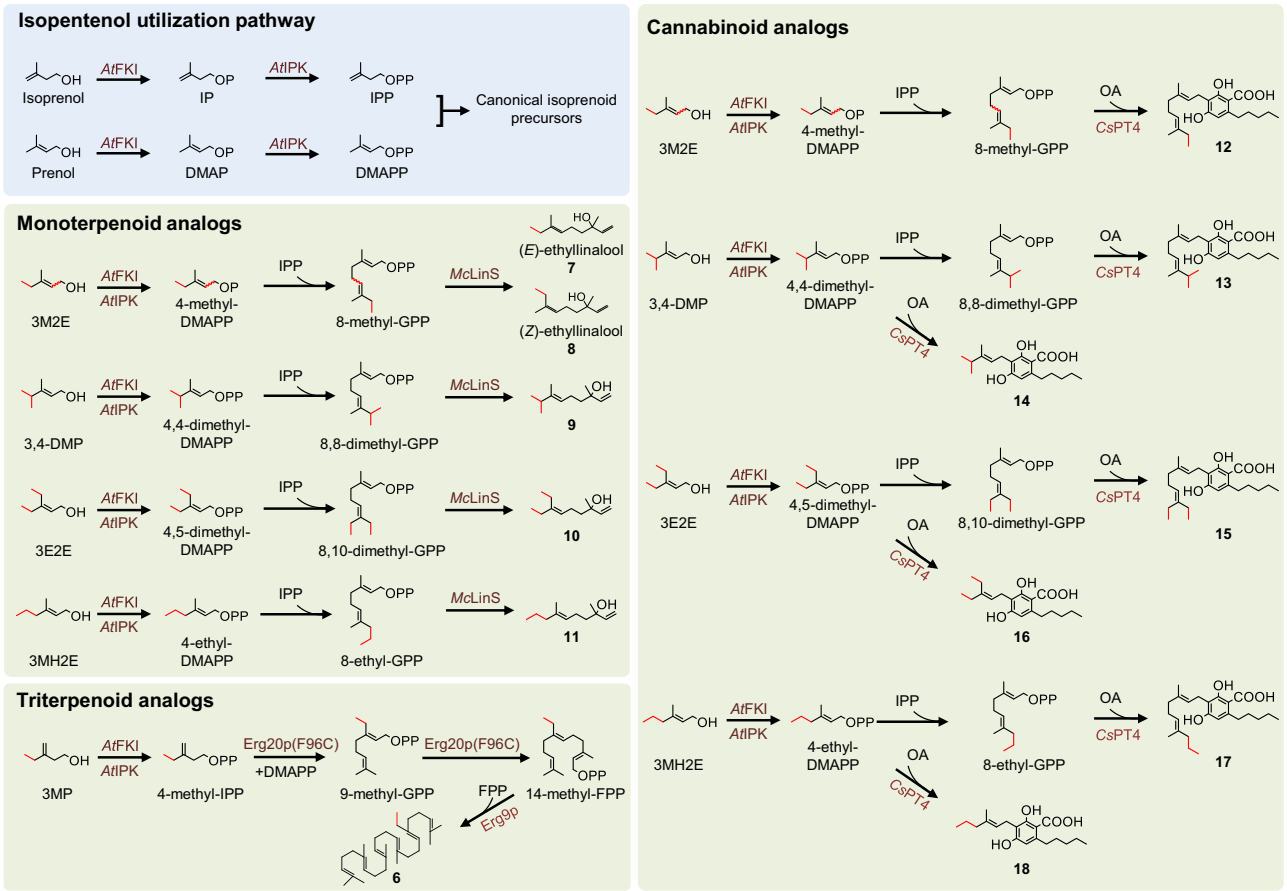

Fig. 1 | Overview of the developed approach. The developed isopentenol utilization pathway is shown in the light blue box. In this pathway, prenol and isoprenol are phosphorylated successively by *At*FKI and *At*IPK to generate DMAPP and IPP, respectively, which are then used to synthesize canonical terpenes. To produce terpenoid analogs, we used seven isopentenol-like alcohols (3M2E, 3MH2E, 3,4-DMP, 3E2E, 3MP, 4E3E and 3MH1E; see main text for full compound names), which can be accepted by *At*FKI and *At*IPK to generate non-canonical terpenoid building blocks (4-methyl-DMAPP, 4-ethyl-DMAPP, 4,4-dimethyl-DMAPP, 4,5-dimethyl-DMAPP, 4-methyl-IPP, 4,5-dimethyl-IPP and 4-ethyl-IPP, respectively). These non-canonical terpenoid building blocks condense with IPP or DMAPP to give rise to non-canonical prenyl diphosphate precursors (e.g., 8-methyl-GPP). Subsequently, terpene synthases or prenyltransferases utilize these non-canonical prenyl diphosphate precursors to produce terpenoid analogs (e.g., ethyllinalool) and high-value compounds (e.g., non-canonical CBGA analogs). OA olivetolic acid.

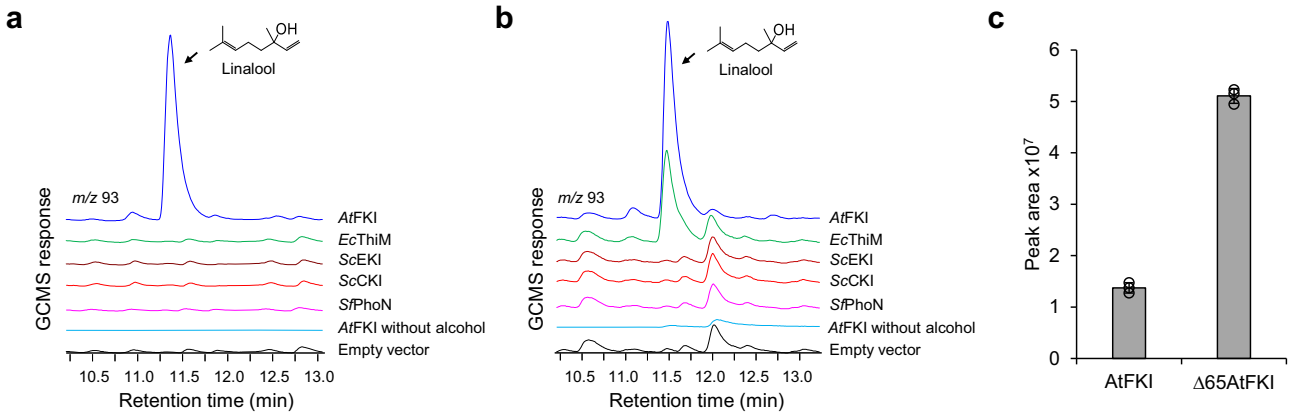

Fig. 2 | Identification of an efficient kinase to support the first step of the constructed isopentenol utilization pathway. Co-expression of kinase candidates and *At*IPK in yeast cells to identify the optimal kinase for the first step of the constructed pathway. Yeast cells containing the empty vectors (strain LW20; black) or yeast cells with *At*IPK and *At*FKI (strain LW01) incubated in the absence of prenol or isoprenol (light blue) are used as controls. **a** Linalool production evaluated by SPME analysis of the headspace of yeast cultures supplied with 0.1% v/v prenol. **b** Linalool production in the headspace of yeast cultures supplied with 0.1% v/v isoprenol. **c** Comparison of linalool production by yeast cells containing the full-length *At*FKI and or the truncated form Δ65*At*FKI and supplied with 0.1% v/v prenol. Values represent the mean of three biological replicates ($n = 3$) and error bars correspond to standard deviation. Source data are provided as a Source Data file.

https://doi.org/10.1038/s41467-025-57494-2

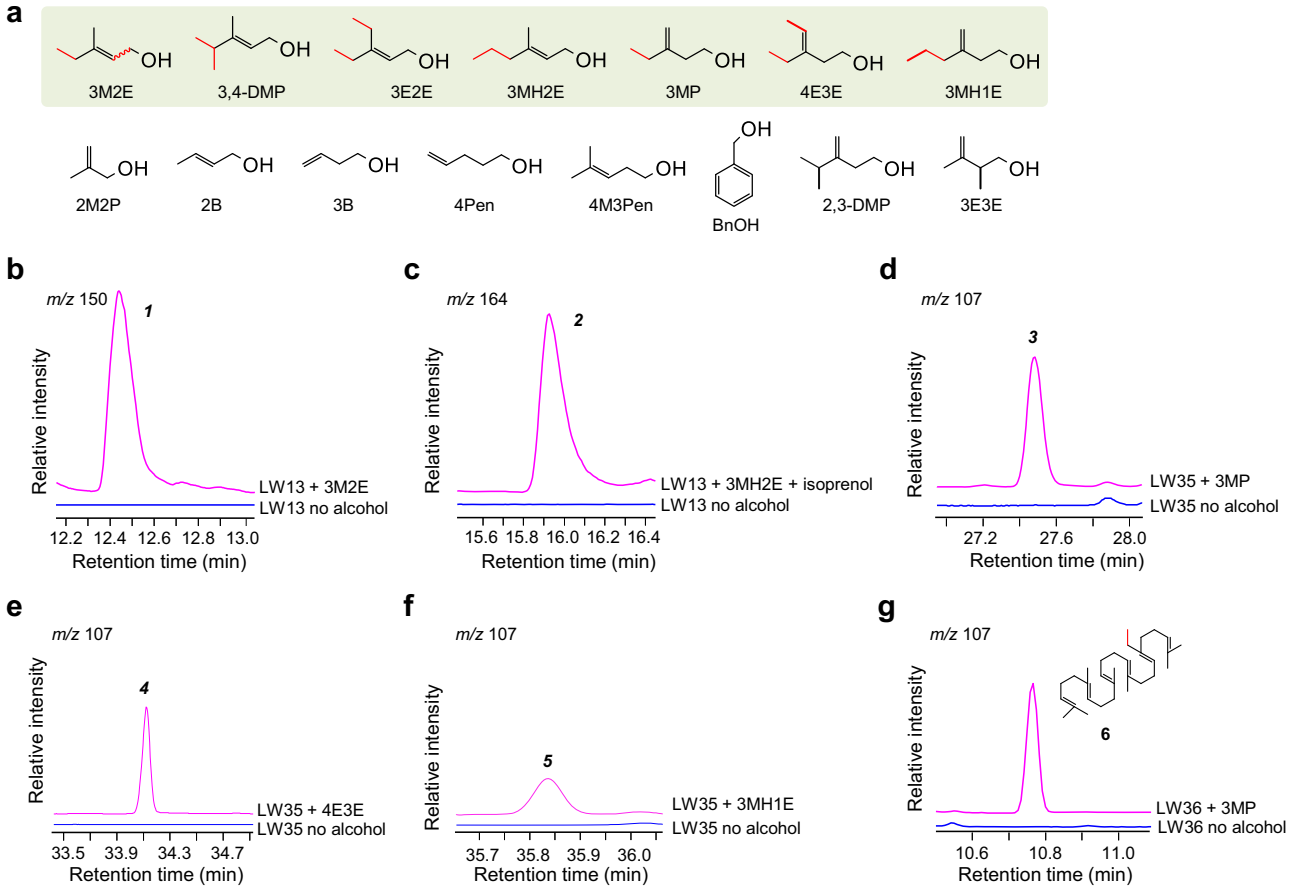

Fig. 3 | Synthesis of monoterpene, sesquiterpene, and triterpene analogs in yeast. a Isopentenol-like alcohols evaluated in this study. Alcohols that were efficiently converted by the established isopentenol utilization pathway into prenyl diphosphate analogs are indicated by a light green box. Structural differences from the corresponding canonical isopentenol are shown in red. **b** SPME-GC-MS extracted ion chromatogram (*m/z* 150; corresponding to $C_{11}H_{18}$) showing the production of ***1*** when the limonene synthase-containing yeast strain LW13 was supplied with 0.01% 3M2E. Strain LW13 incubated in the absence of the corresponding alcohol is shown as a control (blue). **c** SPME-GC-MS extracted ion chromatogram (*m/z* 164; corresponding to $C_{12}H_{20}$) showing the production of ***2*** by LW13 cells supplied with 0.005% v/v 3MH2E and 0.01% v/v isoprenol to facilitate the conversion. **d**–**f** SPME-GC-MS extracted ion chromatogram showing that strain LW35 (co-expressing *Sf*CarS1 and *ERG20(F96C)*) produced one C_{16} analog (***3***) and two C_{17} analogs (***4*** and ***5***) when supplied with 0.05% v/v 3MP, 4E3E, or 3MH1E, respectively, in the presence of 0.05% v/v isoprenol. **g** GC-MS extracted ion chromatogram showing the production of 26-methyl-squalene (***6***) by strain LW36 (co-expressing *ERG9* and *ERG20(F96C)*) when supplied with 0.05% v/v 3MP and 0.05% v/v isoprenol.

in converting prenol (Fig. 2c). Subsequently, we integrated the genes for Δ65*At*FKI and *At*IPK into the genome of the yeast strain EGY48, to ensure stable expression levels for further studies (strain LW12; Supplementary Table 3).

Biosynthesis of prenyl diphosphate analogs

Having established an efficient alternative isoprenoid pathway, we next employed it to generate non-canonical prenyl diphosphate precursors. We searched for commercially available alcohols with structural similarity to isopentenols and identified several candidates (Fig. 3a). To investigate which of these alcohols could be accepted by *At*FKI and *At*IPK to produce prenyl diphosphate analogs, we supplied them individually to strain LW12 and monitored the production of C_{11} or C_{12} terpenes, likely derived from hydrolysis of the diphosphate products. We found that seven of the candidates could be utilized by *At*FKI and *At*IPK to give rise to products with characteristic fragment ions (*m/z* 150 or 164; Supplementary Figs. 2 and 3). These included the six-carbon alcohols 3-methylpent-2-enol (3M2E) and 3-methylidenepentanol (3MP), and the seven-carbon alcohols 3,4-dimethylpent-2-enol (3,4-DMP), 3-ethylpent-2-enol (3E2E), 3-methylhex-2-enol (3MH2E), 3-ethylpent-3-en-1-ol (4E3E) and 3-methylidenehexan-1-ol (3MH1E). These results suggested that the isopentenol-like alcohols were phosphorylated by *At*FKI and *At*IPK to produce the corresponding DMAPP and IPP analogs, which, in turn, were combined with endogenous IPP or DMAPP to give rise to GPP analogs with 11 or 12 carbon atoms (Fig. 1). Acid hydrolysis of these C_{11}-GPP or C_{12}-GPP precursors in the yeast medium resulted in the production of the non-canonical C_{11} or C_{12} terpenoids presented in Supplementary Fig. 2[18,20,21,33]. By determining the level of alcohol consumption, we observed efficient incorporation of prenol-like alcohols into prenyl phosphates, with efficiencies ranging from 62.1% to 95.6% (Supplementary Table 4). Isoprenol-like alcohols showed lower incorporation, between 20.6% and 44.7%, and required higher substrate concentrations for optimal incorporation. The observed preference for prenol-like alcohols likely reflects the natural substrate selectivity of *At*FKI, whose native substrate is a prenol-type alcohol (farnesol). Furthermore, among the prenol-like alcohols, there was no clear preference between 6- and 7-carbon substrates. Within the isopentenol-like category, on the other hand, the 6-carbon alcohol (3MP) was more efficiently incorporated than the 7-carbon options (4E3E and 3MH1E; Supplementary Table 4).

Terpene synthases use the non-canonical precursors

We then set out to utilize the yeast strains synthesizing DMAPP and IPP analogs to produce different classes of isoprenoids, namely monoterpenes, sesquiterpenes, and triterpenes. We first examined the custom synthesis of monoterpene analogs by focusing on limonene. To

produce non-canonical limonene-like molecules, we supplied 3M2E and 3MH2E, two alcohols that could give rise to C_6 and C_7 analogs of DMAPP, to the limonene synthase-containing strain LW13 (Supplementary Table 3). Following GC-MS analysis of 3M2E-supplied cells, one major product, **1**, could clearly be detected, which was presumed to be an 11-carbon terpene by GC-APCI-qToF-HRMS analysis and the characteristic fragment ions observed in its mass spectrum (Fig. 3b and Supplementary Fig. 4). When strain LW13 was supplied with 3MH2E, one C_{12} compound, **2**, was detected (Fig. 3c and Supplementary Fig. 5).

We proceeded to investigate the possibility of applying the same approach to produce sesquiterpene analogs. To evaluate the efficiency of the system, we introduced the terpentetriene synthase (Cyc2) from *Kitasatospora griseola*[36] to facilitate the production and detection of sesquiterpene products (strain LW28; Supplementary Table 3), as previous studies revealed that Cyc2 was able to accept various C_{16} terpene building blocks and synthesize non-canonical terpenes[21]. Following SPME-GC-MS analysis, C_{16} (*m/z* 218) and C_{17} (*m/z* 232) terpenes could be detected when 3,4-DMP, 3M2E, and 3MP, were supplied (Supplementary Figs. 6 and 7). However, the levels of these compounds were low, suggesting that the yeast FPP synthase Erg20p may not be efficient in generating the larger C_{16} and C_{17} building blocks. We reasoned that a GGPP synthase may be more suitable to accommodate the larger size of the intermediates or products. Thus, we examined a series of GGPP synthases from different organisms together with the variant Erg20p(F96C), which functions as a GGPP synthase[27]. Co-expression of Cyc2 with the selected GGPP synthases revealed that Erg20p(F96C) had superior performance in accepting the non-canonical substrates to synthesize C_{16} or C_{17} prenyl diphosphates (Supplementary Fig. 6). Having improved the production of the C_{16} and C_{17} building blocks, we next investigated the possibility to generate specific sesquiterpene analogs. To this end, we focused on *trans-β*-caryophyllene as a representative compound because of its application as a flavoring agent. We co-expressed Erg20p(F96C) and the caryophyllene synthase *Sf*CarS1[37] in strain LW12 and supplied 3M2E, 3,4-DMP, 3E2E, 3MH2E, 3MP, 4E3E, or 3MH1E. We observed three *Sf*CarS1 products, **3, 4**, and **5**, when each of the IPP-like alcohols 3MP, 4E3E, or 3MH1E, respectively, was supplied (Fig. 3d–f and Supplementary Figs. 8–11). As the prenol-like alcohols 3,4-DMP and 3M2E did not yield any *Sf*CarS1 products, although they could be incorporated into C_{16} and C_{17} prenyl diphosphates (Supplementary Fig. 6), we concluded that the prenyl diphosphate analogs synthesized by these alcohols could not serve as substrates for the caryophyllene synthase.

Subsequently, we investigated the production of non-canonical triterpenes focusing on squalene, the common precursor of numerous high-value triterpenoids. To establish the synthesis of squalene analogs, we overexpressed the yeast squalene synthase gene *ERG9* in an Erg20p(F96C)-producing strain, based on the previous results on sesquiterpenes showing that this variant can improve the production of C_{16} and C_{17} building blocks (strain LW36; Supplementary Table 3). When 3MP was supplied, we observed the synthesis of a putative C_{31} squalene product, **6** (Fig. 3g). Following large scale production and isolation, compound **6** was identified as 26-methyl-squalene by analysis of its NMR spectroscopic data (Supplementary Table 5, Supplementary Fig. 12).

Taken together, these findings demonstrated that the established approach can serve as a general strategy for the systematic production of mono-, sesqui- and triterpenoid analogs. While the production of diterpenoid and tetraterpenoid analogs is conceptually feasible with this method, we were not able to generate GGPP analogs using the same approach, likely due to the inability of Erg20p(F96C) to extend the synthesized C_{16} and C_{17} building blocks to the corresponding C_{21} or C_{22} compounds. Further investigation to identify or engineer suitable prenyltransferases could potentially overcome this barrier, enabling the synthesis of diterpenoid and tetraterpenoid analogs.

Bio-based production of ethyllinalool and linalool analogs with altered sensory characteristics

We next investigated whether this whole-cell biocatalytic method could be applied to produce non-canonical high-value compounds on demand using two case studies. The first case we focused on was the linalool analog 3,7-dimethylnona-1,6-dien-3-ol (commercially known as ethyllinalool). Linalool is widely used in perfumes, cosmetics, food and beverage flavors, and household products due to its pleasant aroma. Ethyllinalool has certain advantages over linalool, such as sweeter and less woody notes, and lower evaporation rate. In Europe alone, the annual registration of ethyllinalool is between 1000 and 10,000 tones[38]. However, ethyllinalool can only be synthesized chemically as a mixture of geometric isomers. Flavor and fragrance ingredients can be obtained from natural sources or chemically synthesized. Generally, those obtained from natural sources (plants or microorganisms) are highly sought after and command a higher price. As ethyllinalool has until now only been available through chemical synthesis, we aimed to develop an alternative method to produce ethyllinalool from a microbial source, as a bio-based product.

Ethyllinalool is an analog of linalool with a methyl group at C-8. Using a simple retrobiosynthetic rationale, we postulated that ethyllinalool could be synthesized from 8-methyl-GPP through the action of a linalool synthase. The precursor, 8-methyl-GPP, could in turn be synthesized from 4-methyl-DMAPP and IPP through a prenyltransferase enzyme, while 4-methyl-DMAPP can be derived from 3M2E by *At*FKI and *At*IPK (Fig. 1). To establish this pathway, we introduced the GPP synthase Erg20p(N127W) and the linalool synthase *Mc*LinS from *Mentha citrata* into strain LW12 to establish strain LW37 (Supplementary Table 3). When supplied with a mixture of (*E*)- and (*Z*)-3M2E, strain LW37 generated mainly (*E*)-ethyllinalool, **7**, which was confirmed upon comparison with a commercially available ethyllinalool standard (Fig. 4a) and by NMR analysis of the purified compound (Supplementary Tables 6 and 7, Supplementary Fig. 13). Only minor amounts of (*Z*)-ethyllinalool, **8** (Supplementary Tables 6 and 7, Supplementary Fig. 13), were synthesized, suggesting that the stereoselectivity of Erg20p(N127W) and/or *Mc*LinS could distinguish between the two 8-methyl-GPP isomers produced. Furthermore, we evaluated the efficiency of the reconstructed pathway at different alcohol concentrations and determined that the optimal balance between (*E*)-3M2E conversion and (*E*)-ethyllinalool titer was achieved at 0.003% (v/v) (*E*)-3M2E (Supplementary Fig. 14). At this concentration, 51.5 ± 1.7% of (*E*)-3M2E was converted to (*E*)-ethyllinalool, obtaining a product titer of 21.94 ± 0.73 mg/L (Supplementary Table 8).

The sensory characteristics of the produced and isolated (*E*)-ethyllinalool (**7**) and (*Z*)-ethyllinalool (**8**) were evaluated by a professional flavorist and were found to be significantly distinct. (*E*)-Ethyllinalool was found to be fruity and floral, with a strong impact, while (*Z*)-ethyllinalool was considerably less impactful, with prominent agrestic notes (Fig. 4e). This analysis revealed that (*E*)-ethyllinalool is the desirable odor-active component among the two isomers and demonstrated that the biotechnological method for the production of ethyllinalool results in a superior product consisting almost exclusively of the desirable geometric isomer, while the chemical synthesis-based method produces a mixture of the two isomers.

In addition to demonstrating the bio-based synthesis of ethyllinalool, these results suggested that it is possible to develop further linalool analogs. Thus, by supplying strain LW37 with 3,4-DMP, we were able to produce (*E*)-8,8-dimethyl-linalool (**9**; Fig. 4b) and confirm its identity by NMR analysis (Supplementary Tables 6 and 7, Supplementary Fig. 13). Similarly, by supplying 3E2E and 3MH2E, we were able to synthesize 8,10-dimethyl-linalool (**10**; Fig. 4c) and (E)-8-ethyl-linalool (**11**; Fig. 4d), respectively. The identity of the biosynthesized 8,10-dimethyl-linalool and 8-ethyl-linalool was also confirmed by NMR analysis of the isolated compounds (Supplementary Tables 6 and 7, Supplementary Fig. 13).

https://doi.org/10.1038/s41467-025-57494-2

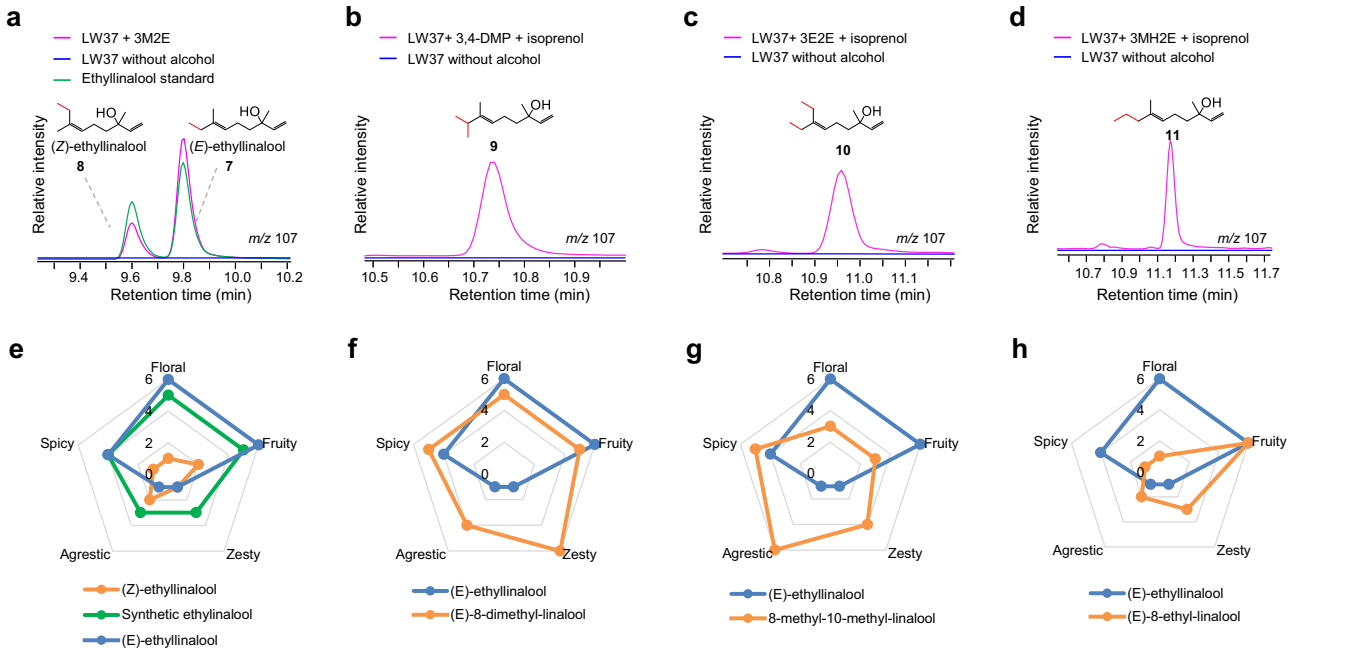

Fig. 4 | Synthesis of ethyllinalool and other linalool analogs in yeast. GC-MS ion-extracted chromatograms (*m/z* 107) of the headspace of strain LW37 grown in the presence of (**a**) 0.01% v/v 3M2E, (**b**) 0.005% v/v 3,4-DMP and 0.01% v/v isoprenol, (**c**) 0.005% v/v 3E2E and 0.01% v/v isoprenol, or (**d**) 0.005% v/v 3MH2E and 0.01% v/v isoprenol, showing the production of ethyllinalool and linalool analogs (pink). An ethyllinalool standard sample is shown in green in panel (**a**). Chromatograms from yeast cells (strain LW37) not supplied with the respective alcohols are shown as controls (blue). The sensory characteristics of each of the isolated linalool analogs were evaluated by a professional flavourist and five quality attributes (floral, fruity, spicy, zesty, and agrestic) were scored in the scale of 1-6 and plotted in the form of a spider diagram (panels **e**–**h**).

For compounds **9**–**11**, we determined the alcohol-to-product conversion and product titer at different alcohol concentrations (Supplementary Fig. 14). Overall, for (*E*)-3M2E, 3E2E, and 3MH2E, the alcohol-to-product conversion was close to the alcohol consumption levels at the corresponding concentrations (Supplementary Table 4). Thus, for these alcohols, the first phosphorylation step of the pathway (*At*FKI) seems to be the most crucial step. In the case of 3,4-DMP, the alcohol-to-product conversion is lower than the alcohol consumption level, suggesting that the substrate preference of the prenyltransferase Erg20p(N127W) or the linalool synthase *Mc*LinS may be a limiting factor.

The three linalool analogs, **9**–**11**, were also evaluated for their sensory characteristics. (*E*)-8,8-dimethyl-linalool (**9**) was found to be zesty, floral, fruity, and spicy, with agrestic notes (Fig. 4f), while 8,10-dimethyl-linalool (**10**) was found to be mainly agrestic, zesty, and spicy, with weak fruity and floral notes (Fig. 4g). (*E*)-8-Ethyl-linalool (**11**) displayed a strong fruity pineapple-like character, with very weak zesty and agrestic notes, and almost no floral character (Fig. 4h). Overall, these results demonstrate that using the proposed methodology it is possible to produce flavoring molecules with altered or improved characteristics that can have specific applications as ingredients.

Cannabinoid analogs with improved cannabinoid receptor activation

Cannabinoids are medicinally important isoprenoids with neuromodulatory and immunomodulatory activities that have the potential to delay the progression of neurodegenerative diseases, such as Alzheimer's, Huntington's, and multiple sclerosis[39,40]. Cannabinoids exert their activity by targeting the human cannabinoid receptors CB_1 and CB_2[41,42]. In the cannabinoid biosynthetic pathway, olivetolic acid (OA) and GPP are condensed by the action of the dedicated geranyl transferase *Cs*PT4 to form cannabigerolic acid (CBGA)[3]. Since cannabinoid analogs bearing modifications on the GPP-derived moiety may exhibit altered bioactivity, we proceeded to investigate the production of cannabinoid derivatives.

To produce CBGA analogs, we developed strain LW16 by incorporating *Cs*PT4 and Erg20p(N127W) into strain LW12 (Supplementary Table 3). We supplied LW16 with OA (0.1 mM) and each of the five isopentenol-like alcohols and analyzed the ethyl acetate extracts of the corresponding yeast cells by UPLC–HRMS for the biosynthesis of CBGA analogs. Four of the alcohols (3M2E, 3,4-DMP, 3E2E, and 3MH2E) gave rise to seven products (**12**–**18**, Fig. 5), likely formed by the condensation of OA with DMAPP or GPP analogs (Fig. 1). To confirm this prediction, we isolated compounds **12**–**18** and elucidated their structures using NMR spectroscopy (Supplementary Tables 9 and 10, Supplementary Fig. 15). 3M2E produced primarily 8′-methyl-CBGA (**12**) (Fig. 5a), while 3,4-DMP produced primarily 8′,8′-dimethyl-CBGA (**13**) and lower amounts of the 4,4-dimethyl-DMAPP-derived compound **14** (Fig. 5b). 3E2E produced mainly 8′,10′-dimethyl-CBGA (**15**) and minor amounts of the 4,5-dimethyl-DMAPP-derived compound **16** (Fig. 5c). Finally, 3MH2E produced equal amounts of 8′-ethyl-CBGA (**17**) and the 4-ethyl-DMAPP-derived compound **18** (Fig. 5d). By examining for production efficiency of the cannabinoid analogs (Supplementary Table 11), it was evident that in the case of the 3,4-DMP-derived compounds **17** and **18**, the obtained product titers and rates of alcohol conversion into product were considerably lower, suggesting that either Erg20p(N127W) is less efficient with 4,4-dimethyl-DMAPP or *Cs*PT4 is less efficient with 8,10-dimethyl-GPP.

Bioactivity evaluation of the cannabinoid analogs

To the best of our knowledge, compounds **12**–**18** are all novel molecules whose synthesis or bioactivities have not been reported before. Thus, to evaluate the bioactivity of the CBGA analogs, we studied their ability to activate the human cannabinoid receptor CB_2. To this end, we employed a yeast cell-based assay that couples the activation of CB_2 to a luminescence reporter[43]. This assay uses yeast cells in which the mating receptor Ste3p and the Gα protein Gpa1p have been replaced by the CB_2 receptor and a chimeric Gpa1p whose last five amino acid residues have been replaced with the corresponding residues of the

https://doi.org/10.1038/s41467-025-57494-2

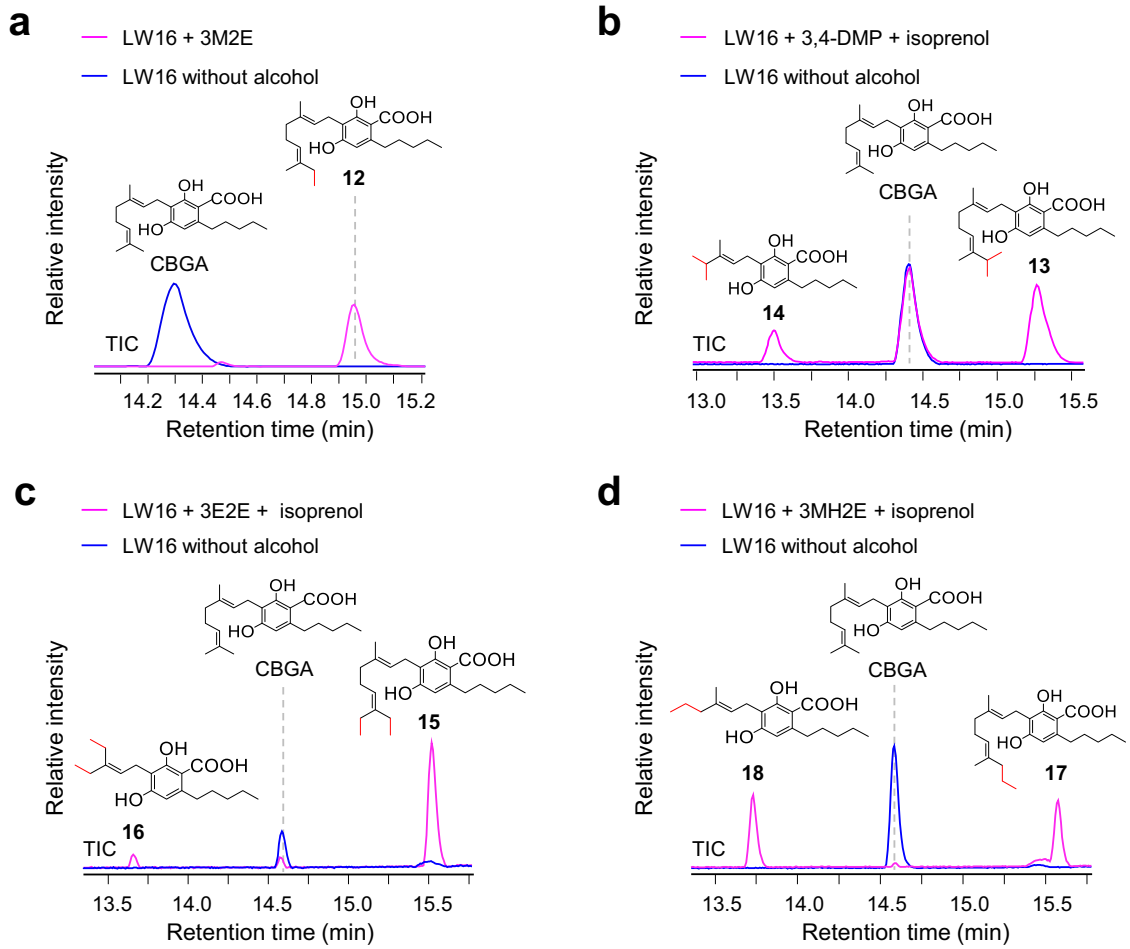

Fig. 5 | Production of CBGA analogs in yeast. UPLC–HRMS analysis of extracts of strain LW16 (containing the geranyl transferase *Cs*PT4) revealed the production of analogs of CBGA (**12**–**18**) (pink), when supplied with 0.5 mM OA and: (**a**) 0.01% v/v 3M2E, (**b**) 0.005% v/v 3,4-DMP and 0.01% v/v isoprenol, (**c**) 0.005% v/v 3E2E and 0.01% v/v isoprenol, or (**d**) 0.005% v/v 3MH2E and 0.01% v/v isoprenol, respectively (total ion chromatograms are shown). LW16 yeast cells supplied only with OA and isoprenol but not any of the prenol-like alcohols are shown as a control (blue). The retention time of CBGA in panels (**a**) and (**b**) differs from panels (**c**) and (**d**) because these experiments were carried out using different instruments.

human CB_2-coupling Gαi. Hijacking the yeast MAP kinase cascade, this system translates CB_2 activation to chemiluminescence through the expression of the nBit luciferase gene. This assay has been shown to enable the facile and robust identification of CB_2 agonists and antagonists in a high-throughput screening format and the discovery of CB_2 ligands present in complex natural extracts[43].

Yeast strain KM206[43] was incubated with a dilution series of compounds **12**–**15, 17**, and **18**, which were isolated in sufficient amounts. Following chemiluminescence quantitative analysis, the obtained dose-response curves revealed that **15** exhibited reduced activation of CB_2 in comparison to canonical CBGA, while **14** and **18** elicited a slight increase (Supplementary Fig. 16). Notably, **12, 13**, and **17** displayed a strong enhancement in bioactivity. Compound **17** demonstrated the most potent effect compared to CBGA, exhibiting a 9.6-fold enhancement of the level of activation at a concentration of 10^{-3} M, while compounds **12** and **13** displayed 8-fold and 7-fold improvement, respectively, at the same concentration (Fig. 6a and Supplementary Table 12). To confirm that the CBGA analogs did not have off-target (non-CB_2-specific) activity, we used a control yeast strain, KM207, that contains an unrelated receptor, in this case the adenosine receptor 2A (A_{2A})[43]. No activation of the A_{2A} receptor was observed by any of the six CBGA analogs (Fig. 6a and Supplementary Fig. 16), suggesting that these ligands did not interfere with non-receptor components of the cell-based assay.

CBGA gives rise to numerous other cannabinoids. One of these compounds is cannabigerol (CBG), which is used in neurological disorders and inflammatory bowel disease[44,45]. Thus, evaluating the bioactivity of CBG analogs holds promise for developing agents with enhanced properties. Previous studies have indicated that CBG can be generated by the decarboxylation of CBGA upon heating[46]. Therefore, we heated the non-canonical CBGA analogs **12**-**15, 17**, and **18** at 99 °C for 3 h. Subsequent UPLC-HRMS analysis revealed that approximately 70–90% of the CBGA analogs had been converted into the corresponding non-canonical CBG analogs. Assessment of the bioactivity of the six heat-treated CBGA analogs using the CB_2 cell-based assay revealed that heat-treated **12, 13**, and **17** demonstrated a significant increase in bioactivity compared to CBG, with an 18.4-fold, 19.1-fold, and 24.4-fold improvement, respectively, at a concentration of 3×10^{-3} M, in comparison to canonical CBG (Fig. 6b and Supplementary Table 12).

Discussion

Here, we develop an efficient and broadly applicable method to generate analogs of isoprenoids, the largest and most diverse group of natural products. Our approach solves a key challenge in the development of isoprenoid analogs with improved properties for applications such as therapeutics, flavors, and fragrances, which could not be addressed by chemical synthesis because the latter requires the

https://doi.org/10.1038/s41467-025-57494-2

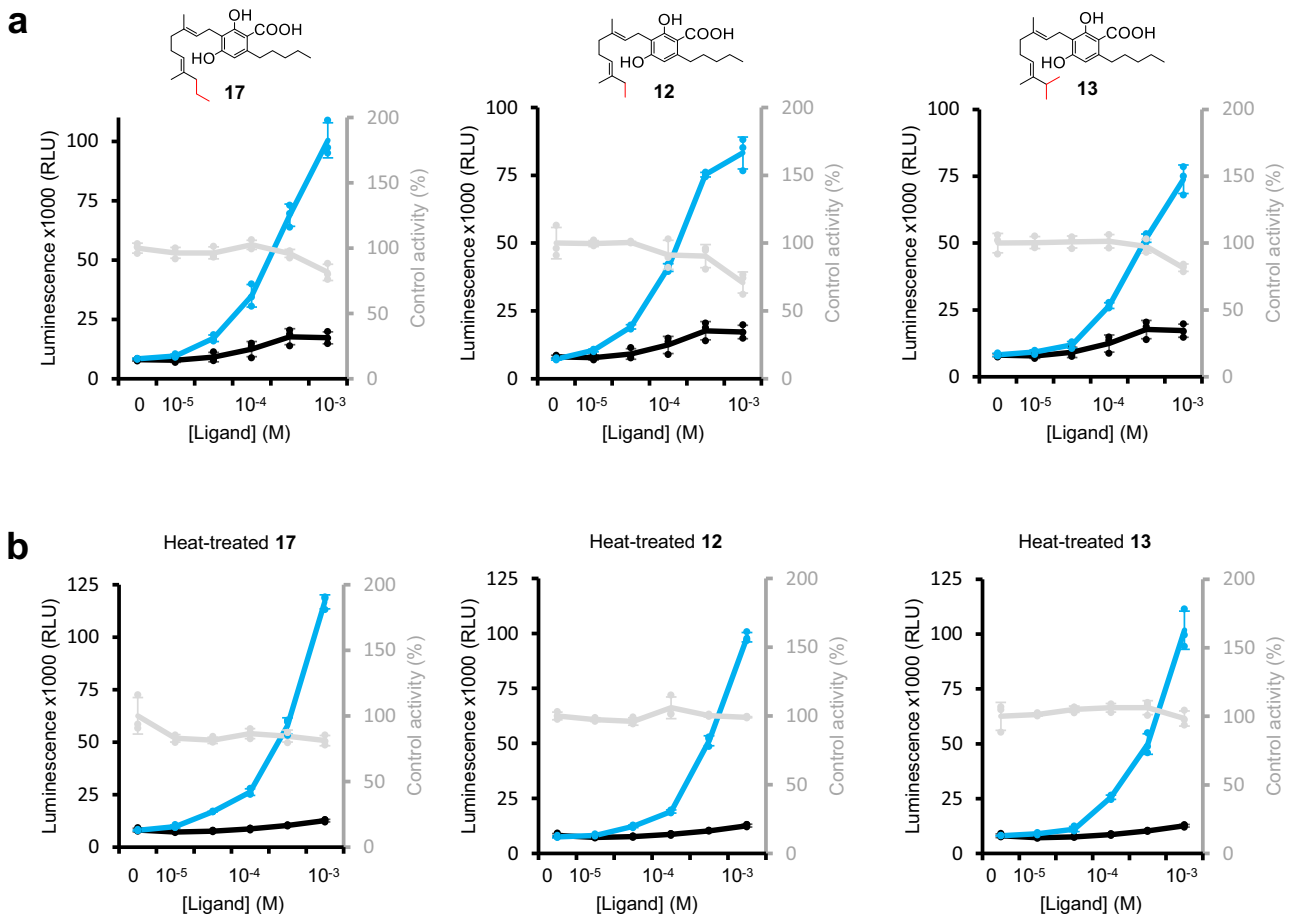

Fig. 6 | Bioactivity evaluation of cannabinoid analogs. a Dose-response curves of the activation of the cannabinoid receptor CB_2 by CBGA and the cannabinoid analogs **12, 13**, and **17** as determined by measuring the resulting luminescent signal using a plate reader. Blue lines indicate the receptor response to the cannabinoid analog, while the black lines show the response induced by CBGA. Gray lines show the response of the control strain expressing the A_{2A} receptor, KM207, to the corresponding cannabinoid analog. **b** Dose-response curves of the activation of CB_2 by CBG and the heat-treated cannabinoid analogs **12, 13**, and **17**. Blue lines indicate the receptor response to the heat-treated cannabinoid analog, while the black lines show the response induced by CBG. Gray lines show the response of the control strain expressing the A_{2A} receptor. Data are represented as the mean of three biological replicates ($n = 3$) and error bars correspond to standard deviation. Source data are provided as a Source Data file.

development of de novo, dedicated, and painstaking synthetic schemes for each compound. The biocatalytic synthesis of isoprenoid analogs using cell factories offers an effective solution, but efforts to date have been constrained by limitations in product diversity, specificity, and yield preventing the efficient production, isolation and functional characterization of analogs.

In earlier studies, the lepidopteran mevalonate pathway, which condenses propionyl-CoA and acetyl-CoA, was introduced into *E. coli* to produce the six-carbon building blocks of homo-IPP (HIPP) and homo-DMAPP (HDMAPP)[47,48]. However, this method was unable to produce dedicated products and channeled the precursors to a multitude of compounds whose structures could not be elucidated. The same challenge was also encountered when a C-methyltransferase was used to synthesize methyl-IPP in bacteria[49]. Other efforts introduced C-methyltransferases into bacterial or yeast cells to convert GPP or FPP into non-canonical substrates for terpene synthases[20,21,50]. However, methyltransferases add only one carbon atom, limiting the chemical diversity of isoprenoids that can be produced. Further limitations stem from the small number of available methyltransferases and their restricted regioselectivity, which limits the diversity of isoprenoid structures accessible via these pathways. An in vitro chemoenzymatic method using purified enzymes to convert prenol-like alcohols to FPP analogs and subsequently to non-canonical terpenoids was also developed[51]. However, this method is not readily scalable and, thus, not suitable for the biotechnological production of isoprenoid analogs for industrial applications.

Unlike previous efforts, the biocatalytic method presented here is specific, enabling the incorporation of one or more carbon atoms at defined positions of the isoprenoid scaffolds, giving rise to tailored molecules. In the examples presented, we demonstrate the addition of a single carbon, two single carbons at distinct positions, and two carbons at one position. While we have showcased the potential of this method using commercially available alcohols, the possibilities can be expanded by synthesizing alcohols with specific modifications or additional carbon atoms. Furthermore, this approach can be adapted to synthesize isoprenoid analogs containing other elements, such as halogens.

This method is systematic and generalizable and can be readily transferred into any existing cell factory for the production of isoprenoids, either prokaryotic or eukaryotic. There are numerous cell factories already developed for isoprenoids[12,22,52,53] which can easily be refactored to produce analogs of the corresponding compounds using the methodology presented here. Furthermore, additional cell factories can be established utilizing the multitude of known isoprenoid biosynthetic pathways. As demonstrated by the two case studies

presented here, this method provides access to a large number of compounds whose synthesis or study was not possible before, while, through coupling with functional assays (bioactivity, sensory, etc.), it enables the facile exploration of the isoprenoid chemical space for molecules with improved characteristics. Moreover, the identified pair of kinases can be introduced into transformable plant, fungal, or bacterial cells to synthesize analogs of the isoprenoids naturally produced in these organisms to expand bioprospecting efforts.

The approach is scalable and economical, limited only by the cost of obtaining or synthesizing the modified alcohols (many of which are available as bulk chemicals at a <10 $/kg price). The efficiency of alcohol conversion and the overall yields of the method are substantial, as demonstrated here by the ability to readily synthesize and isolate sufficient amounts of linalool or cannabinoid analogs for structural elucidation and further functional and bioactivity studies. This performance can be improved further by protein engineering of the isoprenoid biosynthetic enzymes, as several previous studies have established that prenyltransferases and terpene synthases have relaxed substrate specificity which can be expanded further by protein engineering[15,20,21,24–27,33,35,54–56].

Furthermore, by introducing the two key genes, *At*FKI and *At*IPK, into different organisms and supplying appropriate alcohol substrates, our approach enables the production and integration of non-canonical isoprenoids in place of their canonical counterparts, providing an avenue to explore their physiological functions. For example, in yeast cells, it can enable creating non-canonical sterols that can substitute, partly or fully, for canonical sterols in the cell membrane, allowing to systematically examine the effects of non-canonical sterols on membrane integrity, fluidity, and overall yeast physiology. Similarly, introducing this pathway into bacteria would enable to study how isoprenoid analogs influence cell survival, adaptation, or interactions with other microorganisms. Additionally, such bacterial systems could serve as platforms for producing non-canonical isoprenoid-derived natural products to study their roles in microbial ecology. In model plants, the integration of this pathway offers the potential to study the function of terpenoid analogs in plant-insect and plant-microbe interactions. Thus, this method will have applications beyond the biotechnological production of isoprenoids, in natural product chemistry, biochemistry, physiology, and microbiology.

Methods

Chemicals, enzymes and buffers

Standards used include: (*R*)-(+)-limonene (Sigma-Aldrich, 62118), CBGA solution (Sigma-Aldrich, C-142), ethyllinalool (Amitychem), adenosine (Sigma-Aldrich, A9251). Olivetolic acid (FD61416) was purchased from Biosynth. Prenol (162353), isoprenol (129402), 2M2P (2-methyl-2-propenol, 112046), 2B (2-butenol, 244341), 3B (3-butenol, 496839), 4Pen (4-pentenol, 302481) and 4M3Pen (4-methyl-3-pentenol, 311200) were purchased from Sigma-Aldrich. 3M2E (3-methyl-pent-2-enol, EN300-141099), 3,4-DMP (3,4-dimethyl-pent-2-enol, EN300-365161), 3E2E (3-ethylpent-2-enol, EN300-2524336), 3MH2E (3-methyl-hex-2-en-1-ol, EN300-7017978) and 3MP (3-methylidene-pentanol, EN300-371708) were purchased from Enamine MADE BBs. Isopropyl myristate and hexane were purchased from PanReac AppliChem. All chemicals were of reagent grade. Nano-glo luciferase reagent was bought from Promega, US.

DNA restriction enzymes, USER® Enzyme and T4 DNA ligase were obtained from New England Biolabs (Herlev, Denmark) and used according to the manufacturer's instructions. Phusion High-Fidelity DNA polymerase (New England BioLabs, M0530S) and MyTaq DNA polymerase (BIO-21105, Bioline) were used in PCR amplifications. QIAquick Gel Extraction Kit (Qiagen, ID: 28704) was used for gel extraction and DNA purification. QIAprep Spin Miniprep Kit (Qiagen, ID: 27104) was used for plasmid purification.

D-(+)-glucose monohydrate (16301, Sigma), D-(+)-galactose (MG05201, CarboSynth), D-(+)-raffinose pentahydrate (R1030, US Biological), Yeast Nitrogen Base w/o AA (Y2025, US Biological), yeast synthetic drop-out powder without histidine, leucine, tryptophan and uracil (Sigma-Aldrich, Y2001), were used for yeast cultivation.

Gene cloning and expression in yeast

All primers used for cloning purposes are listed in Supplementary Data 1. All plasmid constructions (Supplementary Table 2) were made using the *E. coli* Mach1™ strain (Thermo Fisher Scientific, Roskilde, Denmark).

The kinase genes of *A. thaliana* FKI (*At*FKI; GenBank NM_125242.4), *S. flexneri* (*Sf*PhoN; GenBank BAA11655.1), *S. cerevisiae* CKI (*Sc*CKI; GenBank AAA34499.1), *S. cerevisiae* EKI (*Sc*EKI; SGD S000002554), *T. acidophilum* IPK (*Ta*IPK; GenBank CAC11251.1), *A. thaliana* IPK (*At*IPK; GenBank AAN12957.1), *M. thermautotrophicus* IPK (*Mt*IPK; GenBank AAB84554.1) and terpene synthase genes of yeast codon-optimized versions of *Citrus limon* (*R*)-(+)-limonene synthase (*Cl*LimS; GenBank 424 AF514287.1), *Cannabis sativa* geranyl transferase (*Cs*PT4; GenBank BK010648), *Salvia fruticosa* caryophyllene synthase (*Sf*CarS; GenBank OK356796) and *M. citrata* (*R*)-(+)-linalool synthase (*Mc*LinS; GenBank AAL99381.1) were obtained by gene synthesis (GeneArt, Thermo Fisher Scientific; Supplementary Data 2). *E. coli* ThiM (*Ec*ThiM; Genbank CAD6009679.1) was directly amplified from *E. coli* genomic DNA. The synthetic genes were PCR amplified using corresponding USER-Gene-FP and USER-Gene-RP primers and cloned by uracil-specific-excision-reagent (USER) cloning. Yeast expression vectors (pUUS, pWUS, pLUS, pHUS) allowing uracil, tryptophan, leucine and histidine selection, as well as yeast chromosome integration vectors all containing AsiSI/Nb.BsmI cassettes, were used for cloning. The constructs were confirmed by sequencing.

Transformation procedures

E. coli competent cells were made by the Mix & Go! Kit (Zymo Research) and transformed following the manufacturer's protocol. *S. cerevisiae* strains were transformed using lithium acetate[10]. The transformations were screened using PCR amplification of the relevant gene(s). All yeast strains generated in this study are listed in Supplementary Table 3.

Small-scale production of monoterpenoid and sesquiterpenoid analogs

The selected yeast strains were cultivated overnight in 5 mL liquid glucose media with appropriate amino acids at 30 °C. The overnight pre-culture was pelleted and washed twice with sterilized Milli-Q water to remove all traces of glucose. The washed pellets were transferred to 20 mL glass vials with magnetic screw caps (Mikrolab Aarhus A/S, Denmark), each containing 2 mL of galactose/raffinose media supplemented with the respective alcohols. Yeast cultures were then incubated (30 °C and 150 rpm) for 3 days before being subjected to GC-MS or GC-APCI-qToF-HRMS analysis.

Evaluation of alcohol consumption by engineered yeast cells

To evaluate the consumption of supplied alcohols, yeast cells expressing *At*FKI and *At*IPK (strain LW12) were incubated as above in the presence of varying alcohol concentrations and the amount of alcohol present in the sample at the end of the incubation period was determined by SPME sampling and GC-MS analysis. Parent EGY48 cells (not carrying the *At*FKI and *At*IPK genes) were incubated in parallel in the presence of the same alcohol concentration and also analyzed by SPME/GC-MS at the end of the incubation period. For each alcohol, the consumption was determined by comparing the levels or remaining alcohol between LW12 and EGY48 cells.

Small-scale production and extraction of triterpenoid analogs

Yeast strains were cultured overnight at 30 °C and 150 rpm in selective glucose medium. Each culture was washed two times with sterilized Milli-Q water and then transferred to a 100 mL glass flask containing

10 mL of galactose/raffinose media supplemented with the respective alcohols. Yeast cultures were incubated (30 °C and 150 rpm) for 3 days prior to extraction. The yeast cultures were then centrifuged at 8000 × *g* for 5 min. The obtained pellets were resuspended in 500 μL of 10% KOH in 80% EtOH solution and incubated at 70 °C for 2 h. Samples were cooled at room temperature and overlaid with 300 μL of hexane followed by vigorous vortexing prior to collecting the hexane phase. The extraction was repeated three times and the collected hexane phase (~0.9 mL) was washed three times with water (equal volume) and evaporated down to 100 μL for GC-MS analysis.

Small-scale production and extraction of cannabinoids

Yeast strains were incubated (30 °C and 150 rpm) for 3 days in selective galactose/raffinose media supplemented with 0.1 mM olivetolic acid and the respective tested alcohols. Yeast cultures were then centrifuged at 8000 × *g* for 10 min. The obtained pellets were resuspended in 500 μL of sterilized Milli-Q water, followed by the addition of 100 mg of glass beads. Subsequently, the samples were treated with vigorous vortexing and extracted with a 1:1 mixture of ethyl acetate and formic acid (0.05% v/v). This extraction process was repeated three times, and the ethyl acetate fractions were pooled together and the solvent was evaporated using a SpinVac. The remainders were resuspended in a methanol and formic acid (0.05% v/v) mixture for analysis by LC-MS.

GC-MS analysis conditions

GC-MS analysis was performed on a Shimadzu QP2020 NX (Shimadzu Corp.) single-quadrupole instrument. The GC-MS Solution software (Shimadzu Corp.) was used for data acquisition and quantification.

SPME analysis of monoterpenoids and sesquiterpenoids: Samples, resulting from incubation of the SPME fiber for 30 min over the head space of 2 mL yeast cultures, were directly analyzed by gas chromatography - mass spectrometry (GC-MS). GC-MS analysis was carried on a DB-5 column with helium as the carrier gas at a constant velocity of 30 cm/s, using the following thermal program: initial temperature 40 °C, ramp to 80 °C with a rate of 3 °C/min, ramp to 110 °C with a rate of 30 °C/min, ramp to 130 °C with a rate of 3 °C/min, ramp to 280 °C with a rate of 30 °C/min, and hold for 3 min.

Analysis of hexane extracts containing triterpenoids: Samples were analyzed using a DB-5 column with helium as the carrier gas at a constant velocity of 30 cm/s, using the following temperature program: initial temperature 60 °C, ramp to 300 °C with a rate of 10 °C/min, ramp to 320 °C with a rate of 3 °C/min, hold for 3.5 min.

GC-APCI-qToF-HRMS analysis conditions

The GC-APCI-qToF-HRMS experiments were performed on a Scion 456 GC system coupled to a micrOTOF-Q II (qToF) mass spectrometer (Bruker Daltonics) and an atmospheric pressure chemical ionization source (APCI)[21]. A BR-5ms capillary column (30 m × 0.25 mm ID × 0.25 μm film thickness; Bruker Daltonics) was used for separation with helium as the carrier gas (flow rate 1.0 mL/min). Perfluorotributylamine vapor (PFTBA; Sigma Aldrich) was used for tuning at the beginning of each injection. The thermal program was set as following: initial temperature 60 °C, hold for 1 min, ramp to 280 °C at a rate of 15 °C/min, hold for 3.67 min. Data was acquired using a combination of Compass CDS (Version 3.0.1; Bruker Daltonics), Compass o-TOF Control (Version 3.4, Bruker Daltonics) and Hystar (Version 3.2 SR4, Bruker Daltonics) software, and analyzed using Compass DataAnalysis (Version 4.3, Bruker Daltonics).

LC-MS analysis conditions

LC–MS analysis was performed on a DionexUltiMate® 3000 Quaternary Rapid Separation UHPLC system (ThermoFisher Scientific, Germering, Germany) equipped with a Kinetex XB-C18 column (150 mm × 2.1 mm i.d., 1.7 μm particle size, 100 Å pore size) (Phenomenex, Inc., Torrance, CA, USA). The column was operated at 40 °C, and the flow rate was maintained at 0.3 mL/min. The mobile phases were water (A) and acetonitrile (B), both containing 0.05% formic acid. Separations were performed using the following gradient profile: 0 min, 2% B; 1 min, 2% B; 15 min, 98% B; 18 min, 98% B; 19 min, 2% B; 26 min, 2% B. All data were analyzed using the Data Analysis 4.3 (Bruker Daltonics) software program.

General procedures for isolation and structure elucidation

Vacuum and gravity column chromatographic separations were performed with Kieselgel 60 (Merck, Darmstadt, Germany). Normal-phase HPLC separations were conducted on a Pharmacia LKB 2248 liquid chromatography pump (Pharmacia LKB Biotechnology, Uppsala, Sweden) equipped with an RI-102 Shodex refractive index detector (ECOM spol. s r.o., Prague, Czech Republic), using an Econosphere Silica 10 u (250 × 10 mm, Grace, Columbia, MD, USA) column. Reversed-phase HPLC separations were conducted using an Agilent 1100 liquid chromatography system equipped with a refractive index detector (Agilent Technologies, Waldbronn, Germany), using a Luna 10 u C18(2) 100 A (250 × 10 mm, Phenomenex, Torrance, CA, USA) column. Chiral HPLC separations were conducted on a Waters 515 liquid chromatography pump (Waters, Milford, MA, USA) equipped with an RI-102 Shodex refractive index detector (ECOM spol. s r.o., Prague, Czech Republic) using a Chiralcel OD 10 μm (250 ×10 mm, Daicel Chemical Industries Ltd., Osaka, Japan) column. Thin layer chromatography (TLC) was performed with Kieselgel 60 F_{254} aluminum plates (Merck, Darmstadt, Germany) and spots were detected after spraying with 20% H_2SO_4 in MeOH reagent and heating at 100 °C. NMR spectra were recorded on a Bruker DRX 400 spectrometer (Bruker BioSpin GmbH, Rheinstetten, Germany) or a Varian 600 spectrometer (Varian, Inc., Palo Alto, CA, USA). Chemical shifts are given on a δ (ppm) scale using TMS as an internal standard. The 1D (^{1}H, ^{13}C, and 1D NOE) and 2D (COSY, HSQC, HMBC, NOESY) experiments were performed using standard Bruker or Varian pulse sequences. Low-resolution EI mass spectra were measured on a 5977B mass spectrometer (Agilent Technologies). MSD ChemStation F.01.03.2357 software (Agilent Technologies) was used for low resolution EI-MS data acquisition and spectra analyses. Topspin 4.0.8 (Bruker), MestReC 4.9.9.9 and MestReNova 15.0.0-34764 (Mestrelab Research) software were used for NMR data acquisition and analysis.

Isolation of compounds 6–18

A 2-L culture of LW37 cells (Supplementary Table 3) supplemented with 3MP was centrifuged and the medium was extracted with hexane at room temperature. After separation of the organic layer and evaporation of the solvent in vacuo, the organic extract (194.0 mg) was fractionated by vacuum column chromatography on silica gel, using *n*-hexane with increasing amounts of ethyl acetate as mobile phase, to afford four fractions (1–4). Fraction 1 (*n*-hexane 100%, 13.5 mg) was subjected to normal-phase HPLC, using *n*-hexane (100%) as eluent, and subsequently to reversed-phase HPLC, using acetonitrile (100%) as eluent, to yield **6** (2.0 mg) in pure form.

An ethyllinalool standard sample (Amitychem, 17.9 mg) was repeatedly subjected to chiral HPLC, using n-hexane/iso-propanol (99:1) as eluent, to yield **7** (1.2 mg) and **8** (0.8 mg) in pure form.

A 2-L culture of LW37 cells (Supplementary Table 3) supplemented with 3,4-DMP was centrifuged and the medium was extracted with hexane at room temperature. After separation of the organic layer and evaporation of the solvent in vacuo, the organic extract (194.6 mg) was fractionated by vacuum column chromatography on silica gel, using *n*-pentane with increasing amounts of diethyl ether, and then ethyl acetate, as mobile phase, to afford 10 fractions (1–10). Fraction 9 (100% diethyl ether, 19.8 mg) was submitted to normal-phase HPLC, using *n*-hexane/ethyl acetate (95:5) as eluent, to yield **9** (4.0 mg). Fraction 10 (100% ethyl acetate, 67.9 mg) was fractionated by vacuum

column chromatography on silica gel, using *n*-hexane with increasing amounts of ethyl acetate as mobile phase, to afford 8 fractions (10A-10H), among which fractions 10 C, 10D and 10E (10–20% ethyl acetate in *n*-hexane) were identified as **9** (52.3 mg) in pure form.

A 2-L culture of LW37 cells (Supplementary Table 3) supplemented with 3E2E was centrifuged and the medium was extracted with hexane at room temperature. After separation of the organic layer and evaporation of the solvent in vacuo, the organic extract (47.6 mg) was subjected to vacuum column chromatography on silica gel, using *n*-pentane with increasing amounts of diethyl ether, and then ethyl acetate, as mobile phase, to afford 10 fractions (1–9), among which fractions 7 and 8 (10–20% diethyl ether in *n*-pentane) were identified as **10** (18.5 mg) in pure form.

A 2-L culture of LW37 cells (Supplementary Table 3) supplemented with 3MH2E was centrifuged and the medium was extracted with hexane at room temperature. After separation of the organic layer and evaporation of the solvent in vacuo, the organic extract (85.0 mg) was subjected to vacuum column chromatography on silica gel, using *n*-pentane with increasing amounts of diethyl ether as mobile phase, to afford six fractions (1–6). Fractions 3 and 4 (2–3% diethyl ether in *n*-pentane, 17.4 mg) were subjected to normal-phase HPLC, using *n*-hexane/ethyl acetate (92:8) as eluent, to yield **11** (9.1 mg) in pure form.

A 2-L culture of LW16 cells (Supplementary Table 3) supplemented with 3M2E was centrifuged, and the pellets were resuspended in 15 mL sterilized Milli-Q water. Subsequently, the suspension was subjected to glass bead-beating for 6 min using a 3 mm microtip probe in a soundproof chamber, employing a Branson Digital Sonifier 250 (Branson Ultrasonics, Danbury, CT, USA) operating at a frequency of 20 kHz. The obtained sample was extracted with hexane at room temperature. After separation of the organic layer and evaporation of the solvent in vacuo, the organic extract (2.2 mg) was fractionated by vacuum column chromatography on silica gel, using cyclohexane with increasing amounts of acetone as mobile phase, to afford 3 fractions (1–3), among which fraction 2 was identified as **12** (0.2 mg) in pure form.

A 2-L culture of LW16 cells (Supplementary Table 3) supplemented with 3,4-DMP was collected and extracted as described for LW16 cells supplemented with 3M2E. After separation of the organic layer and evaporation of the solvent in vacuo, the organic extract (2.1 mg) was fractionated by vacuum column chromatography on silica gel, using cyclohexane with increasing amounts of acetone as mobile phase, to afford 3 fractions (1–3), among which fraction 2 was identified as **13** (0.5 mg) in pure form.

A 3-L culture of LW16 cells (Supplementary Table 3) supplemented with 3,4-DMP was collected and extracted as described for LW16 cells supplemented with 3M2E. After separation of the organic layer and evaporation of the solvent in vacuo, the organic extract (29.0 mg) was fractionated by vacuum column chromatography on silica gel, using cyclohexane with increasing amounts of acetone as mobile phase, to afford 8 fractions (1–8). Fraction 6 (30% acetone in cyclohexane, 3.7 mg) was subjected to normal-phase HPLC, using cyclohexane/acetone (10:90) as eluent, to yield **14** (1.0 mg).

A 2-L culture of LW16 cells (Supplementary Table 3) supplemented with 3E2E was collected and extracted as described for LW16 cells supplemented with 3M2E. After separation of the organic layer and evaporation of the solvent in vacuo, the organic extract (78.9 mg) was fractionated by vacuum column chromatography on silica gel, using cyclohexane with increasing amounts of acetone as mobile phase, to afford 7 fractions (1–7), among which fraction 4 was identified as **15** (9.0 mg) in pure form. Fractions 3 (8% acetone in cyclohexane, 15.9 mg), 5 (20% acetone in cyclohexane, 9.4 mg), and 6 (30% acetone in cyclohexane, 3.5 mg) were separately submitted to normal-phase HPLC, using cyclohexane/acetone (10:90) as eluent, to yield **15** (8.9 mg) and **16** (0.8 mg).

A 2-L culture of LW16 cells (Supplementary Table 3) supplemented with 3MH2E was collected and extracted as described for LW16 cells supplemented with 3M2E. Subsequently, the suspension was subjected to glass bead-beating for 6 min using a Branson Digital Sonifier 250 (Branson Ultrasonics, Danbury, CT, USA) operating at a frequency of 20 kHz. The obtained sample was extracted with hexane at room temperature. After separation of the organic layer and evaporation of the solvent in vacuo, the organic extract (59.8 mg) was fractionated by vacuum column chromatography on silica gel, using cyclohexane with increasing amounts of acetone as mobile phase, to afford 8 fractions (1–8). Fractions 5 (20% acetone in cyclohexane, 6.9 mg) and 6 (30% acetone in cyclohexane, 3.1 mg) were separately submitted to normal-phase HPLC, using cyclohexane/acetone (10:90) as eluent, to yield **17** (0.8 mg) and **18** (3.2 mg).

Structure elucidation of the isolated compounds

The chemical structures of compounds **6**–**18** isolated in pure form (Fig. 1) were established on the basis of the homonuclear and heteronuclear correlations observed (Supplementary Figs. 12, 13 and 15) in their HSQC, HMBC, and COSY spectra, while the geometry of their double bond(s) was determined on the basis of the cross-peaks and enhancements observed in their NOESY and 1D NOE spectra, respectively (Supplementary Tables 5–7, 9 and 10, Supplementary Figs. 17–100, Supplementary Note 1 and 2).

Bioactivity evaluation of cannabinoids

Yeast strains (KM206 or KM207)[43] were grown until saturation. Then cells were pelleted by centrifugation and cell density was set to $OD_{600} = 5$ by resuspending in fresh glucose media lacking uracil. Subsequently, 100 µL of yeast cells were dispensed in 96-well plates and the compound tested was added. The cells were then incubated for 3 h at 30 °C with 200 rpm shaking. A 25 µL aliquot of yeast cells from each well was transferred to a black ProxiPlate™ PerkinElmer (#6006270) and mixed with 25 µL of luciferase reagent (CeLytic Y with 4% Nano-glo reagent). After 10 min of incubation, luminescence was measured with Molecular Devices SpectraMax-M5 plate reader and SoftMax Pro 6.2.2 software with 0.5 s integration time.

Data analysis and illustrations

ChemDraw Professional 15.1 (PerkinElmer) was used to draw chemical structures. Microsoft Excel was used for bar charts and graphs and Microsoft Powerpoint was used for the preparation of illustrations.

Reporting summary

Further information on research design is available in the Nature Portfolio Reporting Summary linked to this article.

Data availability

Data supporting the findings of this work are available within the paper and its Supplementary Information files. A reporting summary for this Article is available as a Supplementary Information file. Source data are provided with this paper.

References

1. Zeng, T. et al. TeroKit: A database-driven web server for terpenome research. *J. Chem. Inf. Model.* **60**, 2082–2090 (2020).
2. Paddon, C. J. & Keasling, J. D. Semi-synthetic artemisinin: a model for the use of synthetic biology in pharmaceutical development. *Nat. Rev. Microbiol.* **12**, 355–367 (2014).
3. Luo, X. et al. Complete biosynthesis of cannabinoids and their unnatural analogues in yeast. *Nature* **567**, 123–126 (2019).
4. Paddon, C. J. et al. High-level semi-synthetic production of the potent antimalarial artemisinin. *Nature* **496**, 528–532 (2013).
5. Jiang, B. et al. Characterization and heterologous reconstitution of Taxus biosynthetic enzymes leading to baccatin III. *Science* **383**, 622–629 (2024).

6. Bradley, S. A. et al. Biosynthesis of natural and halogenated plant monoterpene indole alkaloids in yeast. *Nat. Chem. Biol.* **19**, 1551–1560 (2023).
7. Reed, J. et al. Elucidation of the pathway for biosynthesis of saponin adjuvants from the soapbark tree. *Science* **379**, 1252–1264 (2023).
8. Martin, L. B. B. et al. Complete biosynthesis of the potent vaccine adjuvant QS-21. *Nat. Chem. Biol.* **20**, 493–502 (2024).
9. Zhang, J. et al. A microbial supply chain for production of the anti-cancer drug vinblastine. *Nature* **609**, 341–347 (2022).
10. Dusséaux, S., Wajn, W. T., Liu, Y., Ignea, C. & Kampranis, S. C. Transforming yeast peroxisomes into microfactories for the efficient production of high-value isoprenoids. *Proc. Natl. Acad. Sci. USA* **117**, 31789–31799 (2020).
11. Magnard, J. L. et al. Biosynthesis of monoterpene scent compounds in roses. *Science* **349**, 81–83 (2015).
12. Choi, K. R. & Lee, S. Y. Systems metabolic engineering of microorganisms for food and cosmetics production. *Nat. Rev. Bioengineering.* **1**, 832–857 (2023).
13. Miettinen, K. et al. The ancient CYP716 family is a major contributor to the diversification of eudicot triterpenoid biosynthesis. *Nat. Commun.* **8**, 14153 (2017).
14. Ignea, C. et al. Reconstructing the chemical diversity of labdane-type diterpene biosynthesis in yeast. *Metab. Eng.* **28**, 91–103 (2015).
15. Jia, M., Mishra, S. K., Tufts, S., Jernigan, R. L. & Peters, R. J. Combinatorial biosynthesis and the basis for substrate promiscuity in class I diterpene synthases. *Metab. Eng.* **55**, 44–58 (2019).
16. Frey, M. et al. Combinatorial biosynthesis in yeast leads to over 200 diterpenoids. *Metab. Eng.* **82**, 193–200 (2024).
17. Lee, S. et al. Herbivore-induced and floral homoterpene volatiles are biosynthesized by a single P450 enzyme (CYP82G1) in *Arabidopsis*. *Proc. Natl. Acad. Sci. USA* **107**, 21205–21210 (2010).
18. Duan, Y. T. et al. Widespread biosynthesis of 16-carbon terpenoids in bacteria. *Nat. Chem. Biol.* **19**, 1532–1539 (2023).
19. Jiang, J., He, X. & Cane, D. E. Biosynthesis of the earthy odorant geosmin by a bifunctional Streptomyces coelicolor enzyme. *Nat. Chem. Biol.* **3**, 711–715 (2007).
20. Ignea, C. et al. Synthesis of 11-carbon terpenoids in yeast using protein and metabolic engineering. *Nat. Chem. Biol.* **14**, 1090–1098 (2018).
21. Ignea, C. et al. Expanding the terpene biosynthetic code with non-canonical 16 carbon atom building blocks. *Nat. Commun.* **13**, 5188 (2022).
22. Vickers, C. E., Williams, T. C., Peng, B. & Cherry, J. Recent advances in synthetic biology for engineering isoprenoid production in yeast. *Curr. Opin. Chem. Biol.* **40**, 47–56 (2017).
23. Lund, S., Hall, R. & Williams, G. J. An artificial pathway for isoprenoid biosynthesis decoupled from native hemiterpene metabolism. *ACS Synth. Biol.* **8**, 232–238 (2019).
24. Lund, S., Courtney, T. & Williams, G. J. Probing the substrate promiscuity of isopentenyl phosphate kinase as a platform for hemiterpene analogue production. *Chembiochem* **20**, 2217–2221 (2019).
25. Yoshikuni, Y., Ferrin, T. E. & Keasling, J. D. Designed divergent evolution of enzyme function. *Nature* **440**, 1078–1082 (2006).
26. Kampranis, S. C. et al. Rational conversion of substrate and product specificity in a Salvia monoterpene synthase: structural insights into the evolution of terpene synthase function. *Plant Cell* **19**, 1994–2005 (2007).
27. Ignea, C. et al. Efficient diterpene production in yeast by engineering Erg20p into a geranylgeranyl diphosphate synthase. *Metab. Eng.* **27**, 65–75 (2015).
28. Chatzivasileiou, A. O., Ward, V., Edgar, S. M. & Stephanopoulos, G. Two-step pathway for isoprenoid synthesis. *Proc. Natl. Acad. Sci. USA* **116**, 506–511 (2019).
29. Meadows, A. L. et al. Rewriting yeast central carbon metabolism for industrial isoprenoid production. *Nature* **537**, 694–697 (2016).
30. Ma, Y., Zu, Y., Huang, S. & Stephanopoulos, G. Engineering a universal and efficient platform for terpenoid synthesis in yeast. *Proc. Natl. Acad. Sci. USA* **120**, e2207680120 (2023).
31. Clomburg, J. M., Qian, S., Tan, Z., Cheong, S. & Gonzalez, R. The isoprenoid alcohol pathway, a synthetic route for isoprenoid biosynthesis. *Proc. Natl. Acad. Sci. USA* **116**, 12810–12815 (2019).
32. Gyuris, J., Golemis, E., Chertkov, H. & Brent, R. Cdi1, a human G1 and S phase protein phosphatase that associates with Cdk2. *Cell* **75**, 791–803 (1993).
33. Ignea, C., Pontini, M., Maffei, M. E., Makris, A. M. & Kampranis, S. C. Engineering monoterpene production in yeast using a synthetic dominant negative geranyl diphosphate synthase. *ACS Synth. Biol.* **3**, 298–306 (2014).
34. Fitzpatrick, A. H., Bhandari, J. & Crowell, D. N. Farnesol kinase is involved in farnesol metabolism, ABA signaling and flower development in Arabidopsis. *Plant J.* **66**, 1078–1088 (2011).
35. Liu, Y., Yan, Z., Lu, X., Xiao, D. & Jiang, H. Improving the catalytic activity of isopentenyl phosphate kinase through protein coevolution analysis. *Sci. Rep.* **6**, 24117 (2016).
36. Hamano, Y. et al. Functional analysis of eubacterial diterpene cyclases responsible for biosynthesis of a diterpene antibiotic, terpentecin. *J. Biol. Chem.* **277**, 37098–37104 (2002).
37. Ignea, C. et al. Positive genetic interactors of HMG2 identify a new set of genetic perturbations for improving sesquiterpene production in Saccharomyces cerevisiae. *Microb. Cell Fact.* **11**, 162 (2012).
38. https://echa.europa.eu/registration-dossier/-/registered-dossier/13181/1/2 (2025)
39. Riva, N. et al. Safety and efficacy of nabiximols on spasticity symptoms in patients with motor neuron disease (CANALS): a multicentre, double-blind, randomised, placebo-controlled, phase 2 trial. *Lancet Neurol.* **18**, 155–164 (2019).
40. de Lago, E., Moreno-Martet, M., Cabranes, A., Ramos, J. A. & Fernández-Ruiz, J. Cannabinoids ameliorate disease progression in a model of multiple sclerosis in mice, acting preferentially through CB1 receptor-mediated anti-inflammatory effects. *Neuropharmacology* **62**, 2299–2308 (2012).
41. Matsuda, L. A., Lolait, S. J., Brownstein, M. J., Young, A. C. & Bonner, T. I. Structure of a cannabinoid receptor and functional expression of the cloned cDNA. *Nature* **346**, 561–564 (1990).
42. Munro, S., Thomas, K. L. & Abu-Shaar, M. Molecular characterization of a peripheral receptor for cannabinoids. *Nature* **365**, 61–65 (1993).
43. Miettinen, K. et al. A GPCR-based yeast biosensor for biomedical, biotechnological, and point-of-use cannabinoid determination. *Nat. Commun.* **13**, 3664 (2022).
44. Nachnani, R., Raup-Konsavage, W. M. & Vrana, K. E. The pharmacological case for cannabigerol. *J. Pharmacol. Exp. Ther.* **376**, 204–212 (2021).
45. Sepulveda, D. E. et al. Cannabigerol (CBG) attenuates mechanical hypersensitivity elicited by chemotherapy-induced peripheral neuropathy. *Eur. J. Pain.* **26**, 1950–1966 (2022).
46. Wang, M. et al. Decarboxylation study of acidic cannabinoids: A novel approach using ultra-high-performance supercritical fluid chromatography/photodiode array-mass spectrometry. *Cannabis Cannabinoid Res.* **1**, 262–271 (2016).
47. Eiben, C. B. et al. Mevalonate pathway promiscuity enables non-canonical terpene production. *ACS Synth. Biol.* **8**, 2238–2247 (2019).
48. Pang, B. et al. Lepidopteran mevalonate pathway optimization in *Escherichia coli* efficiently produces isoprenol analogs for next-generation biofuels. *Metab. Eng.* **68**, 210–219 (2021).
49. Drummond, L. et al. Expanding the isoprenoid building block repertoire with an IPP methyltransferase from *streptomyces monomycini*. *ACS Synth. Biol.* **8**, 1303–1313 (2019).

50. Kschowak, M. J., Wortmann, H., Dickschat, J. S., Schrader, J. & Buchhaupt, M. Heterologous expression of 2-methylisoborneol / 2 methylenebornane biosynthesis genes in *Escherichia coli* yields novel C11-terpenes. *PLoS One* **13**, e0196082 (2018).
51. Johnson, L. A., Dunbabin, A., Benton, J. C. R., Mart, R. J. & Allemann, R. K. Modular chemoenzymatic synthesis of terpenes and their analogues. *Angew. Chem. Int. Ed. Engl.* **59**, 8486–8490 (2020).
52. Nielsen, J. & Keasling, J. D. Engineering cellular metabolism. *Cell* **164**, 1185–1197 (2016).
53. Keasling, J. et al. Microbial production of advanced biofuels. *Nat. Rev. Microbiol.* **19**, 701–715 (2021).
54. Greenhagen, B. T., O'Maille, P. E., Noel, J. P. & Chappell, J. Identifying and manipulating structural determinates linking catalytic specificities in terpene synthases. *Proc. Natl. Acad. Sci. USA* **103**, 9826–9831 (2006).
55. Ignea, C. et al. Overcoming the plasticity of plant specialized metabolism for selective diterpene production in yeast. *Sci. Rep.* **7**, 8855 (2017).
56. Ignea, C. et al. Orthogonal monoterpenoid biosynthesis in yeast constructed on an isomeric substrate. *Nat. Commun.* **10**, 3799 (2019).

Acknowledgements

We are grateful to Dr. Simon Dusséaux (University of Copenhagen) for assistance with cannabigerolic acid analysis and Dr. Feiyan Liang (University of Copenhagen) for critical reading of the manuscript. We thank Jack Olsen and Dr. Mariela Ramirez (University of Copenhagen) for their assistance in running analytical instruments. This work was financially supported by the Novo Nordisk Foundation grants NNF19OC0055204 and NNF22OC0080100, and the Independent Research Fund Denmark grant 4258-00065B (to S.C.K.). Work at the National and Kapodistrian University of Athens was supported by the grant no. 20226 (to E.I.). L.W. acknowledges the China Scholarship Council for a PhD scholarship (CSC Grant No. 201909370090).

Author contributions

S.C.K. conceived the study. L.W., M.R., E.I., and S.C.K. designed experiments. L.W., M.R., and Y.Z. conducted all cloning, engineering of *S. cerevisiae*, and chromatographic data analysis. L.W. and M.H.R. performed large-scale yeast cultivation and extraction. A.K., M.H., and E.I. conducted the isolation of terpenoid analogs from yeast cultures and carried out the NMR analysis. L.W., N.L., and K.M. evaluated the bioactivity of cannabinoid analogs. A.F. evaluated the sensory characteristics of linalool analogs. L.W., Y.Z., K.M., I.P., E.I., and S.C.K. wrote the manuscript. All authors read and commented on the final version of the manuscript.

Competing interests

L.W., M.R., and S.C.K. are co-inventors of a patent application (WO2023006699A1) describing the use of *At*FKI to phosphorylate a primary alcohol to a mono- or pyrophosphate terpenoid precursor. A.F. is an employee of EvodiaBio ApS. S.C.K. has financial interests in EvodiaBio ApS. The remaining authors declare no competing interest.

Additional information

Supplementary information The online version contains supplementary material available at https://doi.org/10.1038/s41467-025-57494-2.

Correspondence and requests for materials should be addressed to Efstathia Ioannou or Sotirios C. Kampranis.

Peer review information *Nature Communications* thanks Xiaozhou Luo, Antonios Makris and the other, anonymous, reviewer(s) for their contribution to the peer review of this work. A peer review file is available.